

LIQUID PHASE METHANOL LAPORTE PROCESS DEVELOPMENT UNIT:
MODIFICATION, OPERATION, AND SUPPORT STUDIES

Topical Report

Task 3.2: CO₂ Effects on Methanol
Productivity in the LPMEOH Process

Contractor

AIR PRODUCTS AND CHEMICALS, INC.
Allentown, PA 18195

and

Subcontractor to Air Products

CHEM SYSTEMS INC.
Tarrytown, NY 10591

5 October 1990

Prepared for the United States Department of Energy
Under Contract No. DE-AC22-87PC90005
Contract Period 9 April 1987 - 9 October 1990

DISCLAIMER

This report was prepared as an account of work sponsored by the United States Government. Neither the United States nor the United States Department of Energy, nor any of their employees, makes any warranty, express or implied, or assumes any legal liability or responsibility for the accuracy, completeness, or usefulness of any information, apparatus, product, or process disclosed, or represents that its use would not infringe privately owned rights. Reference herein to any specific commercial product, process, or service by trade name, mark, manufacturer, or otherwise, does not necessarily constitute or imply its endorsement, recommendation, or favoring by the United States Government or any agency thereof. The views and opinions of authors expressed herein do not necessarily state or reflect those of the United States Government or any agency thereof.

TABLE OF CONTENTS

	<u>PAGE</u>
LIST OF TABLES	i
LIST OF FIGURES	ii
ABSTRACT	iii
INTRODUCTION	1
OBJECTIVES	2
PATENT SITUATION	3
SAFETY	3
REGULATORY MATTERS	3
FUTURE PROGRAMS	4
ACKNOWLEDGMENT	4
EXPERIMENTAL	4
1. Materials	4
2. Apparatus	5
3. Operation	6
RESULTS	8
1. Effect of CO ₂ Concentration in CO-Rich Gas Matrix	8
2. Effect of H ₂ O Addition	10
3. Effect of H ₂ O Addition for Shell Gasifier Gas	12
DISCUSSION	13
1. Effect of CO ₂ Concentration	13
2. Effect of H ₂ O Addition	18
SUMMARY AND CONCLUSIONS	22
REFERENCES	24

LIST OF TABLES

	<u>PAGE</u>
TABLE 1 - Feed gas compositions.	27
TABLE 2 - Feed mol% CO ₂ , exit mol% CO ₂ , and CH ₃ OH production rate at 5,000 GHSV.	28
TABLE 3 - Feed mol% CO ₂ , exit mol% CO ₂ , and CH ₃ OH production rate at 10,000 GHSV.	29

LIST OF FIGURES

	<u>PAGE</u>
FIGURE 1 - Schematic of reactor system.	30
FIGURE 2 - The dependence of CH ₃ OH production rate on the feed CO ₂ concentration in the Texaco gasifier gas matrix.	31
FIGURE 3 - The dependence of CH ₃ OH production rate on the exit CO ₂ concentration in the Texaco gasifier gas matrix.	32
FIGURE 4 - The influence of GHSV on CH ₃ OH production rate and exit CO ₂ concentration for the 0% CO ₂ feed gas.	33
FIGURE 5 - The dependence of the measured CH ₃ OH production rate and the calculated equilibrium CH ₃ OH production rate on the exit CO ₂ concentration in the Texaco gasifier gas matrix.	34
FIGURE 6 - The dependence of CH ₃ OH production rate on feed H ₂ O concentration for CO-rich gas (13% CO ₂).	35
FIGURE 7 - The dependence of CH ₃ OH production rate on feed H ₂ O concentration for 0% CO ₂ feed gas.	36
FIGURE 8 - The dependence of CH ₃ OH production rate on feed H ₂ O concentration for 0% CO ₂ feed gas at 225°C.	37
FIGURE 9 - The dependence of CH ₃ OH production rate on feed H ₂ O concentration for the 4% CO ₂ feed gas.	38
FIGURE 10 - The dependence of CH ₃ OH production rate on feed H ₂ O concentration for the 8% CO ₂ feed gas.	39
FIGURE 11 - The dependence of CH ₃ OH production rate on the feed H ₂ O concentration for Shell gasifier gas.	40

0682N

ABSTRACT

In April 1987, Air Products and Chemicals, Inc. started the third and final contract with the U.S. Department of Energy (Contract No: DE-AC22-87PC90005) to develop the Liquid Phase Methanol (LPMEOH*) process. In support of this contract, the effect of CO₂ concentration on the CH₃OH production rate was investigated using a lab-scale autoclave reactor. The feed CO₂ concentration was varied by using feed gases which simulated the composition of Texaco gasifier-derived synthesis gas after addition or removal of CO₂. In addition, since H₂O and CO are readily shifted in-situ to CO₂ and H₂, steam addition was also investigated to complement this study. The CH₃OH production rate was found to be a strong function of CO₂ concentration at a reaction temperature of 250°C. It first increases with increasing feed CO₂ level, passes through a maximum at 8% CO₂, and then decreases with further increase in feed CO₂ up to 17%. With 8% CO₂ in the feed, the CH₃OH production rate at 10,000 stand. lit./kg-hr gas-hourly-space-velocity (GHSV) is approximately 15% higher than that for the base Texaco gasifier gas, suggesting that CO₂ removal from Texaco gasifier gas is a viable means of maximizing CH₃OH productivity. The effect of steam addition on CH₃OH production rate was found to depend on both the feed CO₂ level and GHSV. The feed gases with the low feed CO₂ levels exhibited the most benefit from steam addition. For a particular feed CO₂ concentration, the benefit from steam addition was greater at lower GHSV.

* A trademark of Chem Systems Inc.

INTRODUCTION

The Liquid Phase Methanol (LPMEOH*) process is an efficient process for producing methanol from coal-derived synthesis gas. In the LPMEOH reactor, the methanol synthesis catalyst in a powder form is suspended in an inert liquid medium. Because of the superior heat transfer characteristics of this slurry medium, the highly exothermic and equilibrium-limited methanol synthesis reaction can be run under essentially isothermal conditions. This enables the use of unshifted feed gases which contain high levels of CO and the achievement of a high per-pass conversion.

Methanol productivity from the LPMEOH reactor depends on many factors. One of these factors is feed gas composition. Coal-derived synthesis gas contains mainly CO, CO₂, and H₂, though the relative proportions of these gases depend upon the gasifier design and the gasifier operating conditions. For example, the offgas from a typical Texaco gasifier contains approximately 51% CO₂, 35% H₂, 13% CO, and 1% N₂ + CH₄ by volume. Much of the past work in our laboratory has been done using this gas composition, the so-called CO-rich gas.

Investigations reported in the literature indicate that the concentration of CO₂ in the synthesis gas has a large influence on the CH₃OH synthesis rate. Some studies indicate that the CH₃OH synthesis rate is maximized at a certain CO₂ level. These results are interesting since they suggest the

*A trademark of Chem Systems Inc.

possibility of adjusting the CO_2 content of a synthesis gas stream in order to maximize CH_3OH productivity. For example, CO_2 could be removed from a synthesis gas stream using a known technology such as adsorption.

OBJECTIVES

The primary objective of the present study was to determine the effect of CO_2 concentration in the Texaco gasifier gas matrix on the CH_3OH production rate from a LPMEOH reactor. To this end, feed gases were chosen that simulate the composition of CO-rich gas (Texaco gasifier) after addition or removal of CO_2 . In addition, since H_2O and CO are readily shifted in-situ to CO_2 and H_2 , the effects of H_2O addition were also investigated. Also, the effect of H_2O addition to a feed gas of composition representative of that from a Shell gasifier was investigated. Since the gas from a Shell gasifier is low in CO_2 and H_2 , the motivation in studying the effects of H_2O addition was the possibility of favorably adjusting the reactor gas composition.

A secondary objective of the present study was to expand the experimental data base for the LPMEOH process. Extensive data on product distributions and reaction kinetics for the variety of feed gas conditions used in this study provide essential input for the development of a reaction kinetic model for the LPMEOH process.

PATENT SITUATION

An idea proposal entitled "Use of Steam Addition and/or CO₂ Adjustment to Maximize Methanol Production" was filed (I-C2071). A patent strategy has yet to be finalized, but it will most likely focus on a process control invention. The results from the present study provide necessary input for the development of a reaction kinetic model which will be a key part of the process control scheme.

SAFETY

The major safety concerns in this experimental study were the flammability of H₂ and the toxicity and flammability of CO. The primary measures taken to minimize the consequences of an unexpected release of these gases were: the apparatus was housed in a continuously ventilated walk-in hood and the atmosphere in the hood and the laboratory area were continuously monitored by flammable gas and CO detectors that were interfaced to an automatic gas flow shutdown system.

REGULATORY MATTERS

None applicable.

FUTURE PROGRAMS

The data generated in this study will provide necessary input in the development of a reaction kinetic model for the LPMEOH process. The model development work, which is part of the LP-III research program (Subtask 3.5), is ongoing.

All of the results in the present study were obtained using the BASF S3-85 catalyst, which has been replaced by BASF S3-86 as the superior LPMEOH catalyst. Therefore, additional experimental work will also be done under Subtask 3.5 in order to expand the data base of the BASF S3-86 catalyst.

ACKNOWLEDGMENT

The author would like to thank T. A. Dahl for his excellent work in operating the reactor system and obtaining reliable data. In addition, J. J. Lewnard and T. H. Hsiung provided very valuable guidance throughout this study.

EXPERIMENTAL

Materials:

The catalyst used for these experiments was BASF S3-85-44, a powdered Cu/ZnO/Al₂O₃ methanol catalyst.

The slurring liquid used was either Witco 70 or Drakeol 10 oil, both of which are inert hydrocarbon oils.

Premixed gases, supplied from cylinders or a tube trailer, were obtained from Air Products Specialty Gases. The compositions of these mixtures are shown in Table 1. As stated earlier, the feed gas compositions were chosen to simulate the composition of CO-rich gas (Texaco gasifier) after withdrawal or addition of CO₂. In addition, a gas composition representative of that from a Shell gasifier, which has a low CO₂ content, was also included in the study.

Apparatus:

A schematic of the apparatus is shown in Figure 1. The reactor used was a 316 stainless steel stirred autoclave (Autoclave Engineers) with a 1 liter internal volume. Feed gas was compressed by a gas booster pump. Gas flow rate to the reactor was controlled by an electronic mass flow controller. The vapor product stream was passed through a gas-liquid separator to remove entrained and vaporized oil from the reactor. The gas-liquid separator, the heat-traced lines downstream of the reactor, and the line to the gas chromatograph were maintained at a temperature of 120°C in order to prevent the condensation of product CH₃OH. Reactor pressure was regulated by means of a back pressure regulator and product gas flow rate was measured using a wet test meter.

For some of the experiments, H_2O was added to the feed as steam. This was done using a syringe pump which injected liquid H_2O to a feed preheater located immediately upstream of the reactor inlet. The feed preheater, an electrically-heated vessel packed with stainless steel pieces, vaporized the injected liquid H_2O into the feed gas stream.

Feed and product gas compositions were measured on-line by a GC equipped with a thermal conductivity detector. Since the GC did not adequately resolve the H_2O peak, quantitative analysis for H_2O was not possible. GC analysis for H_2 was done using a palladium transfer tube along with N_2 carrier gas.

Operation:

For all of the experimental runs, the concentration of unreduced catalyst in the slurry was 15% by weight. This was obtained by mixing 60 g of as-received BASF S3-85 catalyst with 340 g of oil. The slurry was then transferred to a charging vessel and injected, with the aid of compressed N_2 , into the autoclave via the port for the rupture disk assembly. The agitator speed for all of the experiments was 1200 RPM to eliminate mass transfer limitations.

Catalyst samples were reduced in-situ using the following procedure. After charging the slurry, the reactor was pressurized with N_2 to 100 psig and heated to $100^\circ C$. The flow was then changed to 2% H_2 /98% N_2 at 1000 sccm. This flow rate corresponds to a gas-hourly-space-velocity (GHSV) of 1000 stand. lit./kg oxide catalyst/hr. The reactor was then heated to $200^\circ C$ at $10^\circ C/hr$ while monitoring the exit gas composition. The consumption of H_2 was monitored and adjustments were made in the heating rate to keep the

cumulative H₂ consumption vs. temperature above the required amount as established in previous work (1). After ramping the temperature to 300°C, the reactor was held at 200°C for approximately 15 hours. The temperature was then raised to 240°C at 10°C/hour and held at the temperature for 1 hour.

CO-rich gas (13% CO₂) was introduced at 240°C and the reactor was pressurized to 750 psig and heated to 250°C. The flow was then increased to 5,000 sccm, which corresponds to a GHSV of 5,000 stand. lit./kg-hr. The CH₃OH production rate was high initially and then decreased to an approximately constant value within the first several hours on stream. The initial CH₃OH production rate was approximately 10% higher than the steady-state value. Measurements of the CH₃OH production rate reported in this study were obtained after a minimum of 24 hours on stream with CO-rich gas feed. A reactor charge was typically kept on stream for approximately 300 hours under a variety of feed conditions, although one charge was run for 1000 hours. Periodically during the course of experiments on the various feed gases, CO-rich gas was run at 250°C and 750 psig in order to check the deactivation rate of the catalyst. Generally, the slurry charge was changed out if the measured CH₃OH production rate in CO-rich gas was less than 95% of that after 24 hours on stream. No corrections were applied to the data reported here to account for the time-dependent deactivation.

In the experiments where H₂O was added to the feed, the GHSV, based on the dry feed gas, was kept constant at either 5,000 stand. lit./kg-hr or 10,000 stand. lit./kg-hr. Generally, the feed H₂O concentration was kept below approximately 5 mol%, since previous work in Air Products' lab has shown that

higher H₂O levels can result in an irreversible agglomeration of the catalyst particles and subsequent deactivation.

Except during the in-situ reactions, the total pressure for all experiments was 750 psig and the reaction temperature for most of the runs was 250°C.

RESULTS

Effect of CO₂ Concentration in CO-Rich Gas Matrix:

Figure 2 shows CH₃OH production rate as a function of feed mol% CO₂, in the CO-rich gas (Texaco gasifier) matrix, for GHSV of 5,000 and 10,000 stand. lit./kg-hr. These data are also presented in Tables 2 and 3. The lowest CH₃OH production rate for both 5,000 and 10,000 GHSV was observed for the feed gas which contained 0% CO₂. As the CO₂ content of the feed is increased, the CH₃OH production rate increases dramatically and reaches a maximum at approximately 8% CO₂ for both 5,000 and 10,000 GHSV. The CH₃OH production rate then decreases upon further increase in the feed CO₂ level up to 17% CO₂. It is interesting to note that, for the feed gas containing 0% CO₂, the CH₃OH production rate is approximately the same at both 5,000 and 10,000 GHSV.

Figure 3 shows the dependence of CH₃OH production rate on exit mol% CO₂ for 5,000 and 10,000 GHSV. Since the well-stirred autoclave reactor used in this work behaves as a continuous stirred tank reactor (CSTR), from the viewpoint of reaction kinetics, it is more relevant to consider the CH₃OH production rate as a function of the exit gas composition. The data in

Figure 3 were obtained from the same experiments used to generate Figure 2 and are also presented in Tables 2 and 3. As can be seen in Figure 3, the basic shape of the curves are the same as shown in Figure 2, where the CH_3OH production rate is plotted versus the feed mol% CO_2 . However, the maxima in the CH_3OH production rate are shifted to slightly higher CO_2 content, that is, approximately 9-10 exit mol% CO_2 .

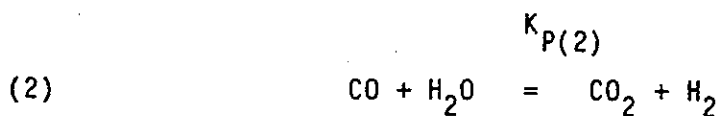
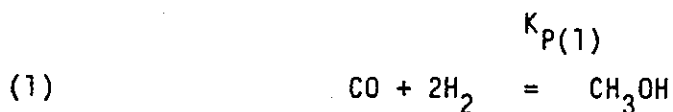
Tables 2 and 3 show that the exit CO_2 concentration, in all cases, is higher than the feed CO_2 concentration. The primary reason for this is that the reactor exit molar flow rate is significantly lower than the feed flow rate owing to the contraction in the total moles resulting from the synthesis of CH_3OH . Generally, material balances across the reactor indicate that little measurable consumption or production of CO_2 occurred in the experiments that did not involve H_2O addition to the feed. However, it is significant to note that, for the 0% CO_2 feed, some CO_2 is produced in the reactor.

Tables 2 and 3 show that the exit CO_2 concentrations at 5,000 and 10,000 GHSV are approximately 0.5% and 0.2%, respectively. The possible explanation for the production of CO_2 from 0% CO_2 feed gas will be discussed later.

Figure 4 shows the influence of GHSV on CH_3OH production rate and exit mol% CO_2 for the 0% CO_2 feed gas. As can be seen, CH_3OH production rate increases with increasing GHSV and approaches an approximately constant value at 5,000 GHSV. As expected, the exit CO_2 concentration decreases with GHSV.

Figure 5 shows the data from Figure 3, CH_3OH production rate versus exit mol% CO_2 , plotted along with calculated equilibrium CH_3OH production rate. In general, the synthesis of CH_3OH from $\text{CO}/\text{CO}_2/\text{H}_2$ is an

equilibrium-limited process. Thus, it is worthwhile to consider the limitations that equilibrium imposes on the CH₃OH production rate. The equilibrium CH₃OH production rate was calculated assuming that the following reactions are at equilibrium:



Values for the equilibrium constants, $K_{P(1)}$ and $K_{P(2)}$, were obtained from reference (2). At 250°C, $K_{P(1)} = 1.65 \times 10^{-3} \text{ atm}^{-2}$ and $K_{P(2)} = 87$.

As shown in Figure 5, the equilibrium CH₃OH production rate decreases with CO₂ concentration. At 5,000 GHSV, the measured CH₃OH production rates at the high CO₂ contents approach the calculated equilibrium line quite closely. By contrast, at 10,000 GHSV, the measured CH₃OH production rates are much less than the calculated equilibrium production rates.

Effect of H₂O Addition:

Since CO₂ can be produced quite effectively in-situ via the water-gas shift reaction, the influence of H₂O addition on CH₃OH production rate was also investigated for some of the feed gases. These results are presented in Figures 6 through 10 in terms of plots of CH₃OH production rate versus feed

mol% H₂O at constant GHSV. The GHSV is based on the dry feed gas, that is, before addition of H₂O.

Figure 6 shows the effect of H₂O addition on CH₃OH production rate for CO-rich gas (13% CO₂). At 5,000 GHSV, added H₂O has a positive effect on CH₃OH production rate. As shown, the addition of 2% and 5% H₂O to the feed resulted in a higher CH₃OH production rate than that for dry gas. The highest CH₃OH production rate at 5,000 GHSV was that for 2% H₂O addition. In contrast, CH₃OH production rate decreases monotonically with increasing feed H₂O concentration for 10,000 GHSV. In fact, the CH₃OH production rate for 8% H₂O in the feed is approximately one-half that for the dry feed gas.

Figure 7 shows the effect of H₂O addition for the 0% CO₂ feed gas. For both 5,000 and 10,000 GHSV, the CH₃OH production rate increases monotonically with increasing feed H₂O concentration over the range 0% to 5% H₂O. The relative increase in CH₃OH production rate with H₂O feed content for 10,000 GHSV is much greater than that for 5,000 GHSV.

The effect of H₂O addition was also determined for the 0% CO₂ feed gas at a temperature of 225°C and 10,000 GHSV. These data are shown in Figure 8. As observed at 250°C, H₂O addition results in an increase in the CH₃OH production rate. However, unlike the results for 250°C, the CH₃OH production rate levels off at approximately 1.5% H₂O.

Results for H₂O addition to the 4% CO₂ and 8% CO₂ feed gases are shown in Figures 9 and 10, respectively. For both feed gases, the CH₃OH production rate is largely unaffected by H₂O addition for either 5,000 GHSV or 10,000 GHSV.

Effect of H₂O Addition for Shell Gasifier Gas:

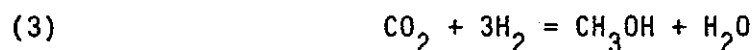
The offgas from a Shell gasifier contains a low concentration of CO₂, typically around 3 mol%. The results presented earlier for the CO-rich gas (Texaco gasifier) matrix show that the maximum CH₃OH production rate occurs at a feed CO₂ level of approximately 8 mol% (Figure 2). However, the corresponding study was not done for Shell gasifier gas. Instead, the effect of H₂O addition to the feed was studied.

Figure 11 shows the effect of H₂O addition for Shell gasifier gas. For both 5,000 and 10,000 GHSV, CH₃OH production rate increases with H₂O feed level up to 5 mol% H₂O. A maximum in the CH₃OH production rate is observed at 5 mol% H₂O addition for 10,000 GHSV, while CH₃OH production rate increases monotonically with feed H₂O level up to 7% H₂O for the 5,000 GHSV case. At 10,000 GHSV, the CH₃OH production rate at the maximum is 15% higher than that for the dry gas.

DISCUSSION

Effect of CO₂ Concentration:

Before discussion of the experimental results, the relevant chemical equations for the synthesis of CH₃OH from CO/CO₂/H₂ mixtures must be considered:



Methanol is produced either by hydrogenation of CO (Equation 1) or by hydrogenation of CO₂ (Equation 3). The water-gas shift reaction, Equation 2, provides a pathway through which CO and CO₂ are interchanged. Only two of these three equations are independent since the third can be formed by a simple combination of the other two.

The role of CO₂ in the synthesis of CH₃OH from CO/CO₂/H₂ mixtures over Cu/ZnO-based catalysts has been the subject of vigorous study in recent years. Although at this point there is probably no general consensus, conclusions drawn from the majority of these studies indicate that hydrogenation of CO₂ is an important, if not dominant, route to CH₃OH synthesis. These conclusions are largely based on studies of CH₃OH synthesis using analysis of reaction products and kinetics (3-8) and isotope labelling studies (7-10). On the other hand, Klier et al. (11) postulate that

CH₃OH is predominantly formed from CO hydrogenation, while the role of CO₂ is to stabilize catalytically active surface Cu⁺¹ species. Finally, some studies conclude that above reactions (1) and (3) are both kinetically important during CH₃OH synthesis at practical conditions (12,13).

The results from the present study do not provide any additional insight as to whether CO or CO₂ hydrogenation is the dominant route to CH₃OH synthesis. The purpose of this study was to establish the effect of feed CO₂ and H₂O levels on the CH₃OH production rate by reaction rate measurements. In general, the elucidation of reaction mechanisms is difficult, if not impossible, using information gathered solely from reaction rate measurements and product analyses. A detailed study using more sophisticated techniques would be required to provide evidence on the specific role of CO₂.

Figures 2 and 3 show that the CH₃OH productivity first increases with CO₂ level, passes through a maximum, and then decreases upon further increase in the CO₂ level. Thus, there is a specific CO₂ level in the Texaco gasifier gas matrix required to maximize the CH₃OH production rate. The maximum CH₃OH production rate occurs at a feed CO₂ level of approximately 8 mol% for both space velocities used. This feed CO₂ level results in approximately 9-10% exit CO₂ concentration. At 10,000 GHSV, the CH₃OH production rate at this CO₂ level is approximately 15% higher than that for CO-rich (13% CO₂) gas.

Similar trends for CH₃OH production rate as a function of CO₂ level for Cu/ZnO-based catalysts have been reported in the literature. Klier et al. (11) studied CH₃OH synthesis in a flow reactor in the temperature range

225-250°C using synthesis gas composed of 70% H₂ and 30% (CO + CO₂). In their experiments, the feed CO₂ and CO levels were varied but the total carbon feed, CO plus CO₂, was kept constant at 30%. Their results show that carbon oxides conversion to CH₃OH increased rapidly with feed CO₂ level up to 2% CO₂, thereafter decreasing upon further increase in CO₂ level. von Wedel et al. (14) also investigated the influence of CO₂ concentration on the CH₃OH rate in a slurry reactor similar to that used in the present study. Their experiments were conducted at reaction temperatures of 217-245°C and were controlled in such a way as to keep the product stream partial pressures of H₂, CO, and CH₃OH constant at 14.8 atm, 9.9 atm, and 2.0 atm, respectively. Their results show that the CH₃OH rate at first increases with reactor CO₂ level, passes through a maximum at approximately 2 atm CO₂, and then decreases with further increase in CO₂ level. The maximum in the CH₃OH rate occurs at approximately 7.2% CO₂. Their results are in very good agreement with those observed in the present study.

In contrast to the above results, Liu et al. (15) found that the initial rate of CH₃OH synthesis in a batch reactor increased monotonically with CO₂ concentration. The experiments of Liu et al. were done at 195°C and 225°C using a gas composition of 70% H₂/30% (CO + CO₂), which is similar to that of Klier et al. (11). The initial rate of CH₃OH production increased with CO₂ level across the range studied, from 1.5% to 30% CO₂. It is important to note, however, that the CH₃OH production rates reported by Liu et al. were initial rates, that is, the rates were measured at conversions much lower than those in the present study.

The reasons for the behavior of the CH_3OH production rate as a function of CO_2 level observed in the present study, the work of Klier et al. (11), and the study of von Wedel et al. (14) is not entirely clear. Despite the fact that CH_3OH synthesis is an extensively investigated subject, details of the complex reaction mechanism and the nature of the active catalytic site are not definitively known. Without such knowledge an attempt to completely explain the observed trend would be highly speculative. Nevertheless, it is worthwhile to consider certain known aspects of the CH_3OH synthesis reaction in an attempt to provide some insight.

In evaluating the effect of gas composition on the CH_3OH production rate, thermodynamic equilibrium limitations must be taken into account. The results in Figure 5 clearly show that equilibrium limits the CH_3OH production rate at low space velocity and high concentrations of CO_2 . However, for the higher space velocity of 10,000 stand. lit./kg-hr, the CH_3OH production rate does not appear to be limited by equilibrium at the high CO_2 levels. Here, it is likely that high CO_2 level reduces the rate of the forward reaction. There are two possible explanations for this effect. Firstly, as feed P_{CO_2} in the Texaco gasifier gas matrix increases, H_2 and CO are replaced, so that P_{H_2} and P_{CO} necessarily decrease. Investigations of the reaction kinetics of CH_3OH synthesis reported in the literature indicate that the reaction rate is largely positive order in P_{H_2} and P_{CO} (8). A reduction in P_{H_2} and P_{CO} would therefore result in a reduction of the CH_3OH synthesis rate. Secondly, at high CO_2 levels, CO_2 may compete with H_2 and/or CO for active sites on the catalyst surface. This competition may decrease the surface concentrations of H_2 and/or CO and could adversely effect the CH_3OH rate.

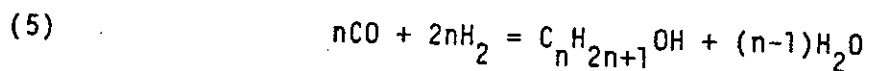
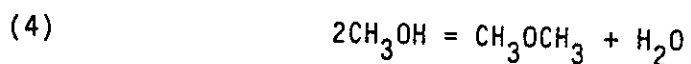
Figures 2 and 3 show that, at the low CO_2 levels, increasing CO_2 content has a strong, positive effect on the CH_3OH production rate. This result is readily understood if CH_3OH is formed primarily from CO_2 hydrogenation. In this case it is reasonable to suppose that, at low CO_2 concentrations, the CO_2 hydrogenation rate is positive order in P_{CO_2} . Another possible explanation for the strong positive effect that increasing CO_2 concentration has on CH_3OH production rate at low CO_2 levels is the previously mentioned idea of Klier et al. (11). Klier et al. explain the positive effect of CO_2 in terms of its influence on the rate of CO hydrogenation. They postulate that CO_2 oxidizes Cu^0 to Cu^{+1} , which is the active site for the hydrogenation of CO . In this scenario, increasing CO_2 concentration would result in more extensive oxidation of Cu^0 to Cu^{+1} , thereby increasing the surface concentration of active sites for CO hydrogenation, resulting in a higher CH_3OH synthesis rate. Clearly, additional investigation is required to determine the fundamentals of the CO_2 effect.

Next, the results obtained with the 0% CO_2 feed gas are considered.

Figures 2 and 3 show that the CH_3OH production rate was lowest for the feed gas with 0% CO_2 . However, as shown in Figure 4, CO_2 was produced in the reactor resulting in exit CO_2 concentrations of 0.2-1.2%, depending on the GHSV. Therefore, in this study, the CH_3OH production rate at 0% CO_2 in the reactor was not determined.

The CO_2 produced in the reactor for the gas containing 0% feed CO_2 most likely originates from the reaction of H_2O and CO via the water-gas shift reaction (reaction (2), above). In this case, the source of the H_2O for the water-gas shift reaction is likely to be the occurrence of non-selective side

reactions. Examples of known side products in the synthesis of CH_3OH are dimethyl ether, methyl formate, and C_{2+} alcohols. The formation of dimethyl ether or C_{2+} alcohols by the following reactions results in the coproduction of H_2O :



Since the equilibrium of the forward water-gas shift reaction (reaction (2)) is very favorable, there exists a large driving force to shift H_2O produced by these side reactions to CO_2 . The result is the presence of CO_2 in the product stream for the 0% CO_2 feed gas. Small quantities (less than approximately 0.1%) of ethanol were observed in the product gas, but accurate quantitative analysis was not possible. The detection of dimethyl ether or alcohols of molecular weight greater than ethanol was not possible with the GC method used.

Effect of H_2O Addition:

It is well known that Cu/ZnO-based CH_3OH synthesis catalysts are also effective catalysts for the water-gas shift reaction. The results obtained for the 0% CO_2 feed gas described above are consistent with this fact. At 250°C , the equilibrium constant for the forward water-gas shift reaction is 87. Therefore, if the reaction rate is sufficiently fast, H_2O added to the Texaco gasifier gas matrix is expected to be shifted with CO almost entirely to CO_2 and H_2 . H_2O addition then provides a means of increasing the

available CO_2 and H_2 at the expense of CO . It is expected then, that the effect of H_2O addition would be analogous to the effect observed upon increasing the CO_2 level in the Texaco gasifier gas matrix. Of course, an additional influence is to be expected as a result of the extra H_2 produced and the CO consumed by the water-gas shift reaction. As stated earlier, investigations of the kinetics of CH_3OH synthesis generally show that the reaction rate orders with respect to P_{H_2} and P_{CO} are positive at practical CH_3OH synthesis conditions. Furthermore, the reaction rate order with respect to P_{H_2} is generally found to be much greater than that for P_{CO} . Thus, an addition in P_{H_2} and corresponding decrease in P_{CO} expected upon H_2O addition should result in a net increase of CH_3OH synthesis rate. An additional consideration in the addition of H_2O is that H_2O may compete with H_2 , CO , and CO_2 for active surface sites, thereby decreasing the hydrogenation rate. With these considerations in mind, the results for H_2O addition can be analyzed.

First, consider the results of the standard Texaco gasifier gas (13% CO_2). H_2O addition results in a decrease in CH_3OH production rate for 10,000 GHSV, but an increase in CH_3OH production rate for 5,000 GHSV (Figure 6). An attempt to explain the effect of H_2O addition to this feed gas must also account for the difference in behavior observed for the two different space velocities. Recall that the results in Figure 2 for the effect of CO_2 content in the Texaco gasifier gas matrix indicate that CO_2 addition to 13% CO_2 feed gas would result in a decrease in the CH_3OH production rate for both 5,000 GHSV and 10,000 GHSV. Since H_2O is shifted to CO_2 , it is expected that H_2O addition to the 13% CO_2 feed gas would decrease the CH_3OH production rate, for either 5,000 GHSV or 10,000 GHSV, on the basis of

the increased CO_2 level. However, the added H_2O also shifts CO to H_2 . Increased H_2 and decreased CO is expected to result in a net increase in CH_3OH production rate, because, as stated earlier, the reaction rate order in P_{H_2} is much more positive than that for P_{CO} . Thus, on the basis of increased H_2 and decreased CO, H_2O addition is expected to increase CH_3OH production rate. Clearly, two opposing influences are operating here: the increased CO_2 content and the increased H_2 content. The reason that H_2O addition is beneficial at 5,000 GHSV but decreases CH_3OH production rate at 10,000 GHSV may be due to a difference in the relative importance of the two opposing influences at the two different space velocities. For example, in the case of 5,000 GHSV, where the conversion of H_2 is relatively high, the increased H_2 available as a result of H_2O addition may have more of an impact on the CH_3OH production rate than the increased CO_2 level. These considerations may account for the differences observed for the two space velocities.

Figure 6 shows that 8% feed H_2O at 10,000 GHSV results in a dramatic suppression of the CH_3OH production rate. Here, the competition of H_2O for surface sites may play a critical role in causing the large decrease in CH_3OH production rate. Another possible reason for the low CH_3OH productivity is that the catalyst may have agglomerated at the high H_2O level as observed in previous work in our laboratory. The exact cause is not known.

The results for H₂O addition to the 0% CO₂ feed gas are considered next. Figure 7 shows that H₂O addition to the 0% CO₂ feed gas is beneficial at both 5,000 and 10,000 GHSV. Here, the CO₂ and H₂ produced in-situ by the shift reaction increase the CH₃OH production rate above that of the dry feed gas. These results are consistent with those in Figure 2, which show the effect of CO₂ concentration. Figure 2 indicates that increasing the CO₂ content of the 0% CO₂ feed gas increases the CH₃OH production rate at both 5,000 GHSV and 10,000 GHSV. By the reasoning presented above, the extra H₂ produced by the shift reaction is also expected to increase the CH₃OH production rate. It is interesting to note that comparison of the CH₃OH production rates in Figure 7 with those of Figure 2 suggests that, at low levels of H₂O addition, H₂O and CO₂ are interchangeable reactants because of the water-gas shift reaction.

Herman et al. (16) and Klier et al. (17) have also observed that addition of low levels of H₂O to CO/H₂ synthesis gas greatly increases the CH₃OH synthesis rate. In contrast, Liu et al. (15) report that H₂O suppresses the initial rate of CH₃OH synthesis in a batch reactor.

Figures 9 and 10 show that the effect of the addition of H₂O to the feed for the 4% CO₂ and 8% CO₂ feed gases is negligible. This observation is consistent with the results of Figure 2, which show that increasing the CO₂ content of either of these feed gases by a small amount should have only a slight effect on CH₃OH production rate.

The results for H₂O addition to Shell gasifier gas (Figure 11) are consistent with the above results for Texaco gasifier gas. Since the Shell gasifier gas has low CO₂ and H₂ concentrations, by the reasoning presented above, the expectation is that increased CO₂ and H₂ levels produced by the in-situ shift of H₂O and CO would increase the CH₃OH production rate.

SUMMARY AND CONCLUSIONS

The effect of CO₂ concentration on the CH₃OH production rate from CO-rich synthesis gas was investigated using a well-stirred slurry reactor. The concentration of CO₂ in the reactor feed gas was varied such that the feed composition was representative of that from a Texaco gasifier with CO₂ addition or withdrawal. Since H₂O and CO are readily shifted in-situ to CO₂ and H₂, the effect of H₂O addition to the feed on CH₃OH production rate was also investigated for several feed gases, including a composition representative of that from a Shell gasifier. The principal conclusions as a result of this study are:

1. Methanol production rate is a strong function of feed CO₂ concentration in the CO-rich gas matrix at 250°C and 750 psig using GHSV of 5,000 and 10,000 stand. lit./kg-hr. The CH₃OH production rate first increases with increasing feed CO₂ level, passes through a maximum at 8% CO₂,

and then decreases with further increase in CO_2 level up to 17% for both 5,000 and 10,000 GHSV. At 10,000 GHSV, the CH_3OH production rate at 8% feed CO_2 is approximately 15% higher than that for CO-rich gas (13% CO_2). These results show that CO_2 removal from CO-rich gas is a means of maximizing CH_3OH production rate.

2. The theoretical equilibrium CH_3OH production rate decreases monotonically with increasing feed CO_2 concentration. At 5,000 GHSV and high feed CO_2 levels, the constraints of thermodynamic equilibrium restrict the CH_3OH production rate. For operation at 10,000 GHSV, restrictions imposed by equilibrium limitations appear to be less important.
3. For a feed gas containing 0% CO_2 , CO_2 is produced in the reactor at an exit level of 0.2–1.2%, depending on the GHSV. The CO_2 in these experiments is believed to be formed from the reaction of CO and H_2O via the water-gas shift reaction. In this case, the source of the H_2O is the occurrence of minor, non-selective reactions, such as the formation of dimethyl ether or C_{2+} alcohols.
4. The effect of H_2O addition on CH_3OH production rate was found to be a function of both feed gas composition and, for a particular feed composition, GHSV. Since H_2O and CO shift readily to CO_2 and H_2 , the effects of added H_2O were interpreted in terms of the increased CO_2 and H_2 content. The feed gases with the lowest CO_2 level

exhibited the maximum benefit from the added H₂O. For the 0% CO₂ feed gas, CH₃OH production rate increased monotonically with H₂O feed concentrations up to 5% for both 5,000 and 10,000 GHSV. Generally, for a particular feed gas, the benefit from H₂O addition was greater at lower GHSV.

5. Addition of H₂O to Shell gasifier gas, which is lean in CO₂ and H₂, resulted in an increase in CH₃OH production rate. At 5,000 GHSV, CH₃OH production rate increases monotonically with feed H₂O levels up to 7%. For operation at 10,000 GHSV, the CH₃OH production rate passes through a maximum at approximately 5% feed H₂O.

REFERENCES

- (1) D. M. Brown, P. Rao, G. W. Roberts, and T. H. Hsiung, U.S. Patent #4,801,574.
- (2) United Catalysts, Inc., "Physical and Thermodynamic Properties of Elements and Compounds."
- (3) B. Denise, R. P. A. Sneed, and C. Hamon, J. Mol. Catal. 17, 359 (1982).
- (4) V. D. Kuznetsov, F. S. Shub, and M. I. Temkin, Kinet. Katal. 23(4), 932 (1982).
- (5) R. Kieffer, E. Ramaroson, A. Deluzarche, and Y. Trambouze, React. Kinet. Catal. Lett. 16(2-3), 207 (1981).

- (6) G. H. Graaf, J. G. M. Winkelman, E. J. Stamhuis, and
A. A. C. M. Beenackers, Chem. Eng. Sci. 43(8), 2161 (1988).
- (7) A. Ya. Rozovskii, Kinet. Katal. 21(1), 97 (1980).
- (8) G. C. Chinchin, P. J. Denny, J. R. Jennings, M. S. Spencer, and
K. C. Waugh, Appl. Catal. 36, 1 (1988).
- (9) G. C. Chinchin, P. J. Denny, D. G. Parker, M. S. Spencer, and D. A. Whan,
Appl. Catal. 30, 333 (1987).
- (10) A. Ya. Rozovskii, G. I. Lin, L. G. Liberov, E. V. Slivinskii,
S. M. Loktev, Yu. B. Kagan, and A. N. Bashkirov, Kinet. Katal. 18(3), 691
(1977).
- (11) K. Klier, V. Chatikavanij, R. G. Herman, and G. W. Simmons, J. Catal. 74,
343 (1982).
- (12) M. Takagawa and M. Ohsugi, J. Catal. 107, 161 (1987).
- (13) G. Liu, D. Willcox, M. Garland, and H. H. Kung, J. Catal. 96, 251 (1985).
- (14) W. von Wedel, S. Ledakowicz, and W.-D. Deckwer, Chem. Eng. Sci. 43(8),
2169 (1988).
- (15) G. Liu, D. Willcox, M. Garland, and H. H. Kung, J. Catal. 90, 139 (1984).

(16) R. G. Herman, K. Klier, G. W. Simmons, B. P. Finn, J. B. Bulko, and
T. P. Kobylinski, *J. Catal.* 56, 407 (1979).

(17) G. A. Vedage, R. Pitchai, R. G. Herman, and K. Klier, *Proc. 8th Int.
Congr. Catal.*, Vol. II, p. 47 (1984).

TABLE 1
FEED GAS COMPOSITIONS

Gas Designation	Requested Mol. %				Average Analysis by GC			
	CO	H ₂	CO ₂	N ₂	CO	H ₂	CO ₂	N ₂
0% CO ₂	58.7	40.3	0.0	1	59.8	38.9	0.0	1.1
2% CO ₂	57.5	39.5	2.0	1	55.9	39.7	2.0	1.1
4% CO ₂	56.3	38.7	4.0	1	54.6	39.7	4.0	1.1
8% CO ₂	54.0	37.0	8.0	1	52.0	38.3	7.9	1.2
CO-Rich	51.0	35.0	13.0	1	50.7	35.8	12.8	1.0
18% CO ₂	48.0	33.0	18.0	1	45.5	34.4	17.1	1.0
Shell Gasifier Gas	66.0	30.0	3.0	1	64.3	31.6	3.0	1.1

Table 2

Feed Mol. % CO₂, Exit Mol. % CO₂, and CH₃OH Production Rate
at 5,000 GHSV

P = 750 psig, T = 250°C, Feed % H₂O = 0

<u>Run No.</u>	<u>Feed % CO₂</u>	<u>Exit % CO₂</u>	<u>CH₃OH Production Rate (gmol/Kg•hr)</u>
10111-13W	0.00	0.57	11.91
10111-13Z	0.00	0.48	11.51
10111-28H	2.00	2.97	18.83
10111-28K	2.00	2.93	17.43
10111-5G	4.07	5.59	18.99
10111-5H	4.07	5.67	19.07
10111-22D	4.07	5.52	17.61
10111-13F	7.84	10.2	19.26
10111-13M	7.91	10.0	18.83
10111-13D	13.0	16.5	16.69
10111-5C	14.6	18.2	16.24
10111-13J	13.0	15.6	16.64
10111-13Q	13.0	17.3	16.47
10111-13S	13.4	16.0	16.24
10111-13U	13.4	15.2	16.46
10111-22A	13.1	16.2	16.25
10111-28B	13.0	15.8	16.28
10111-13B	13.7	16.8	17.30
10111-13C	13.7	17.3	17.39
8975-102A	12.2	15.3	16.37
8975-102D	12.1	16.8	15.7
10111-28N	17.1	20.3	13.8

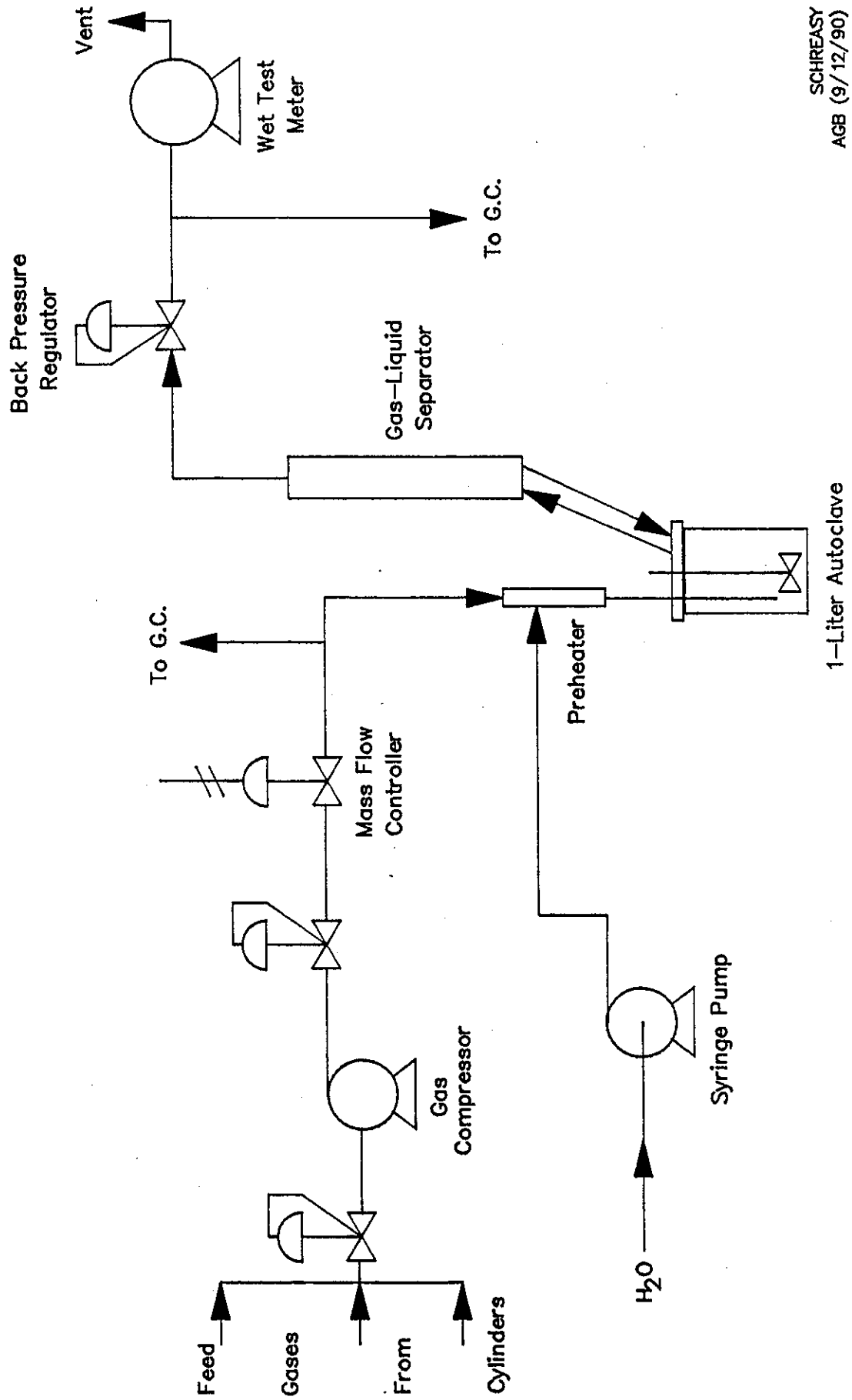
Table 3

Feed Mol.% CO₂, Exit Mol.% CO₂, and CH₃OH Production Rate
at 10,000 GHSV

P = 750 psig, T = 250°C, Feed % H₂O = 0

<u>Run No.</u>	<u>Feed % CO₂</u>	<u>Exit % CO₂</u>	<u>CH₃OH Production Rate (gmol/Kg•hr)</u>
10111-13X	0.00	0.20	12.06
10111-13AC	0.00	0.22	12.60
10111-28I	2.00	2.48	26.39
10111-28J	2.00	2.50	26.64
10111-28L	2.00	2.50	26.72
10111-5I	4.07	5.03	30.77
10111-22I	4.07	4.82	27.59
10111-22E	4.07	4.92	28.45
10111-13G	7.84	9.31	32.24
10111-13L	7.85	9.24	31.12
10111-13E	13.0	14.9	28.75
10111-5D	14.6	15.5	28.10
10111-13AF	13.1	15.8	27.08
10111-13AI	13.1	15.2	26.78
10111-13AN	13.1	15.3	26.27
10111-22B	13.6	15.7	26.22
10111-22C	13.6	15.8	26.04
10111-22S	13.6	14.9	24.45
10111-28C	13.0	15.6	27.24
8975-102B	12.2	14.4	27.73
8975-102F	12.7	14.7	26.71
10111-3G	12.9	14.3	27.59
10111-3H	12.9	14.6	27.56
10111-28M	17.1	19.54	24.06

FIGURE 1: Schematic of Reactor System



SCHREASY
AGB (9/12/90)

FIGURE 2: The dependence of CH_3OH production rate on the feed CO_2 concentration in the Texaco gasifier gas matrix.

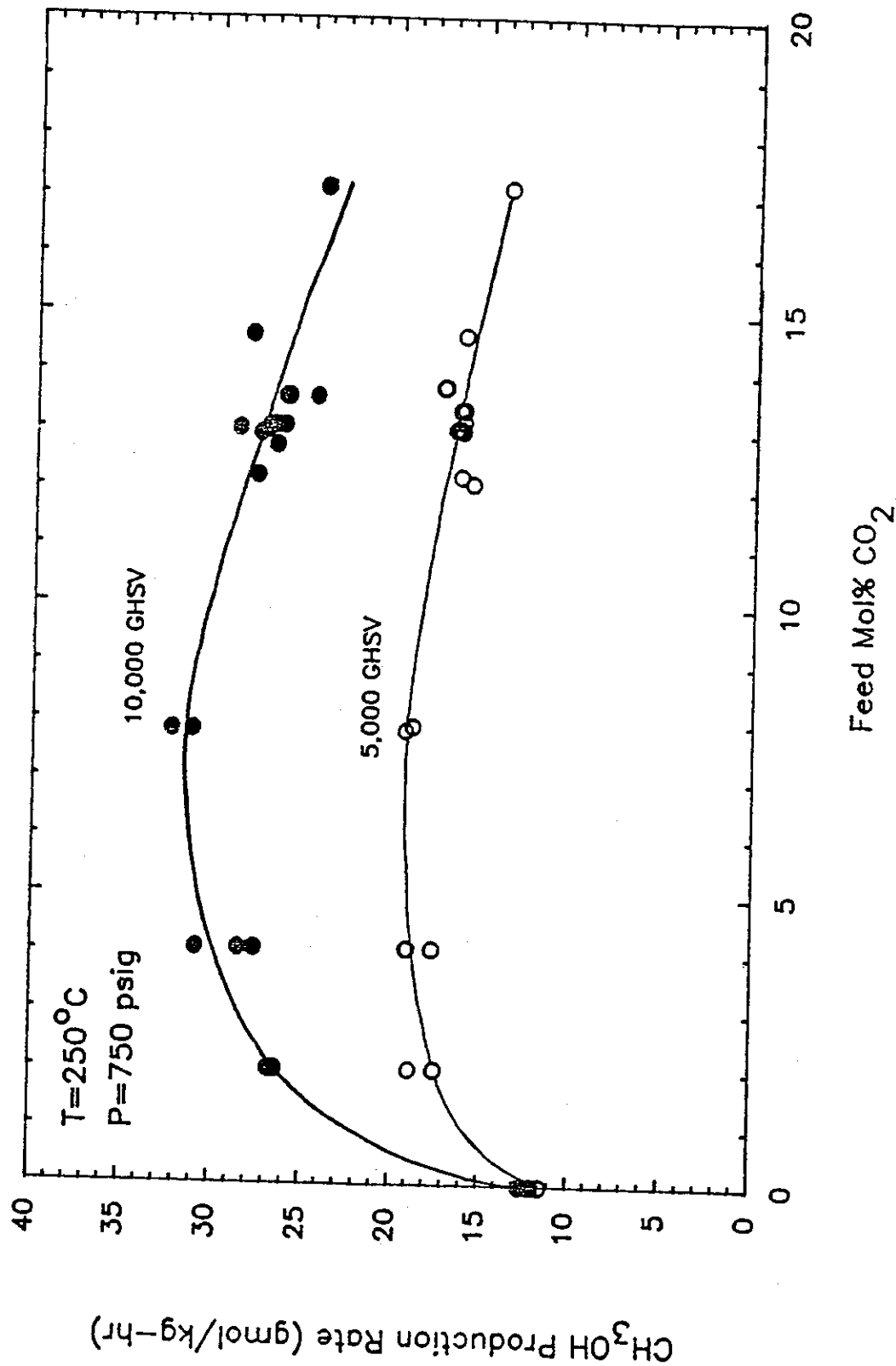


FIGURE 3: The dependence of CH₃OH production rate on the exit CO₂ concentration in the Texaco gasifier gas matrix.

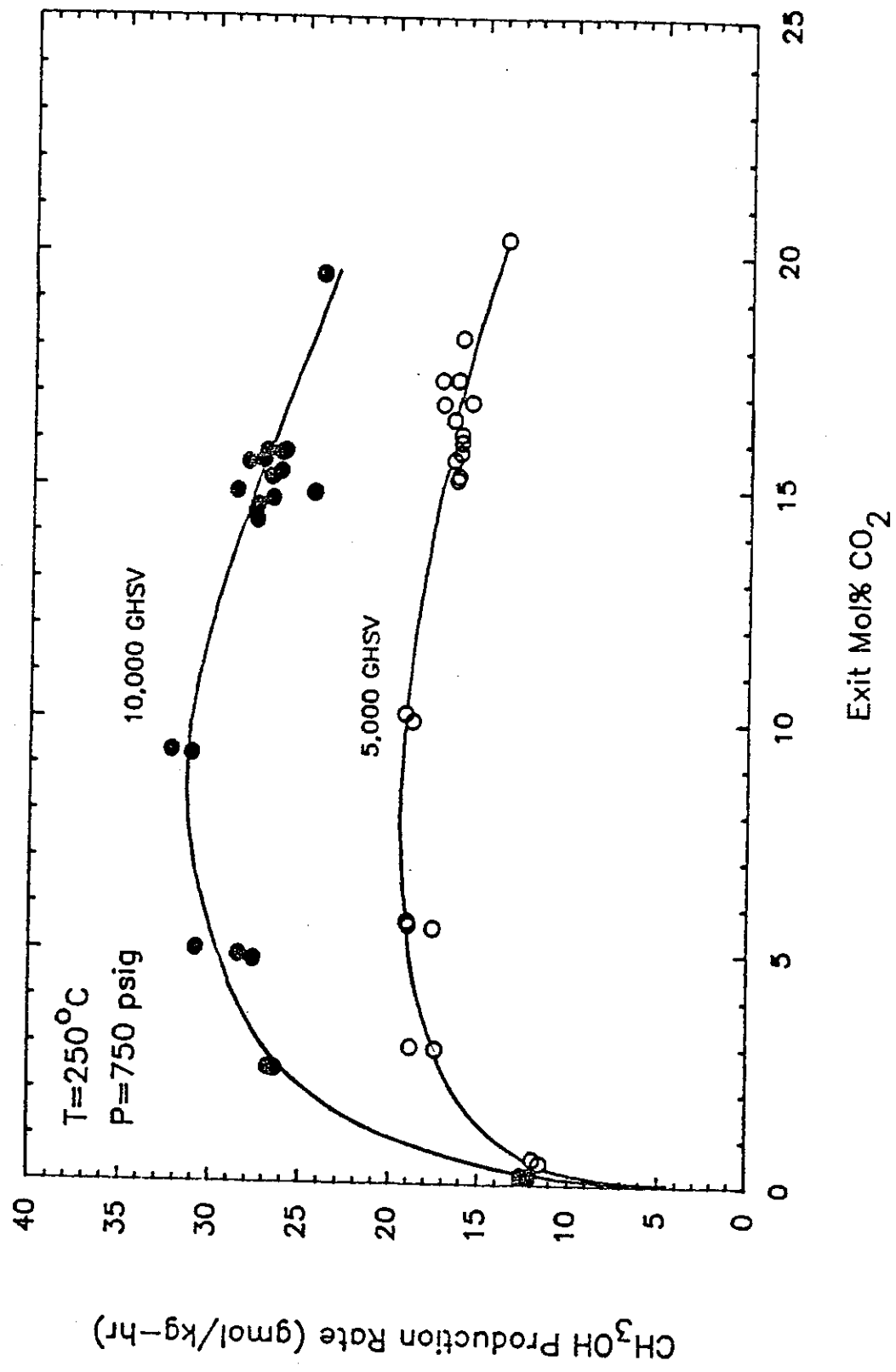


FIGURE 4: The influence of GHSV on CH_3OH production rate and exit CO_2 concentration for the 0% CO_2 feed gas.

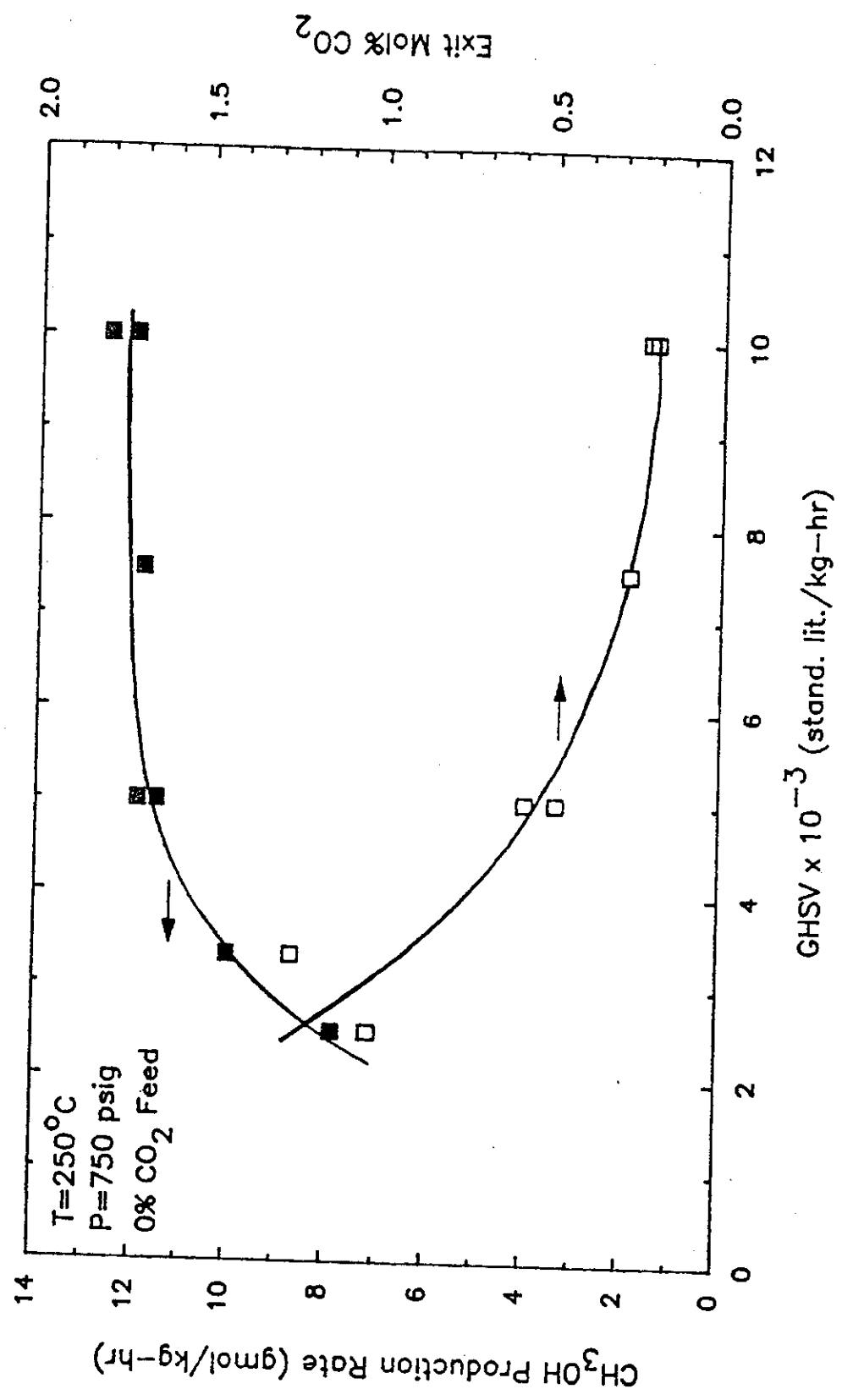


FIGURE 5: The dependence of the measured CH_3OH production rate and the calculated equilibrium CH_3OH production rate on the exit CO_2 concentration in the Texaco gasifier gas matrix.

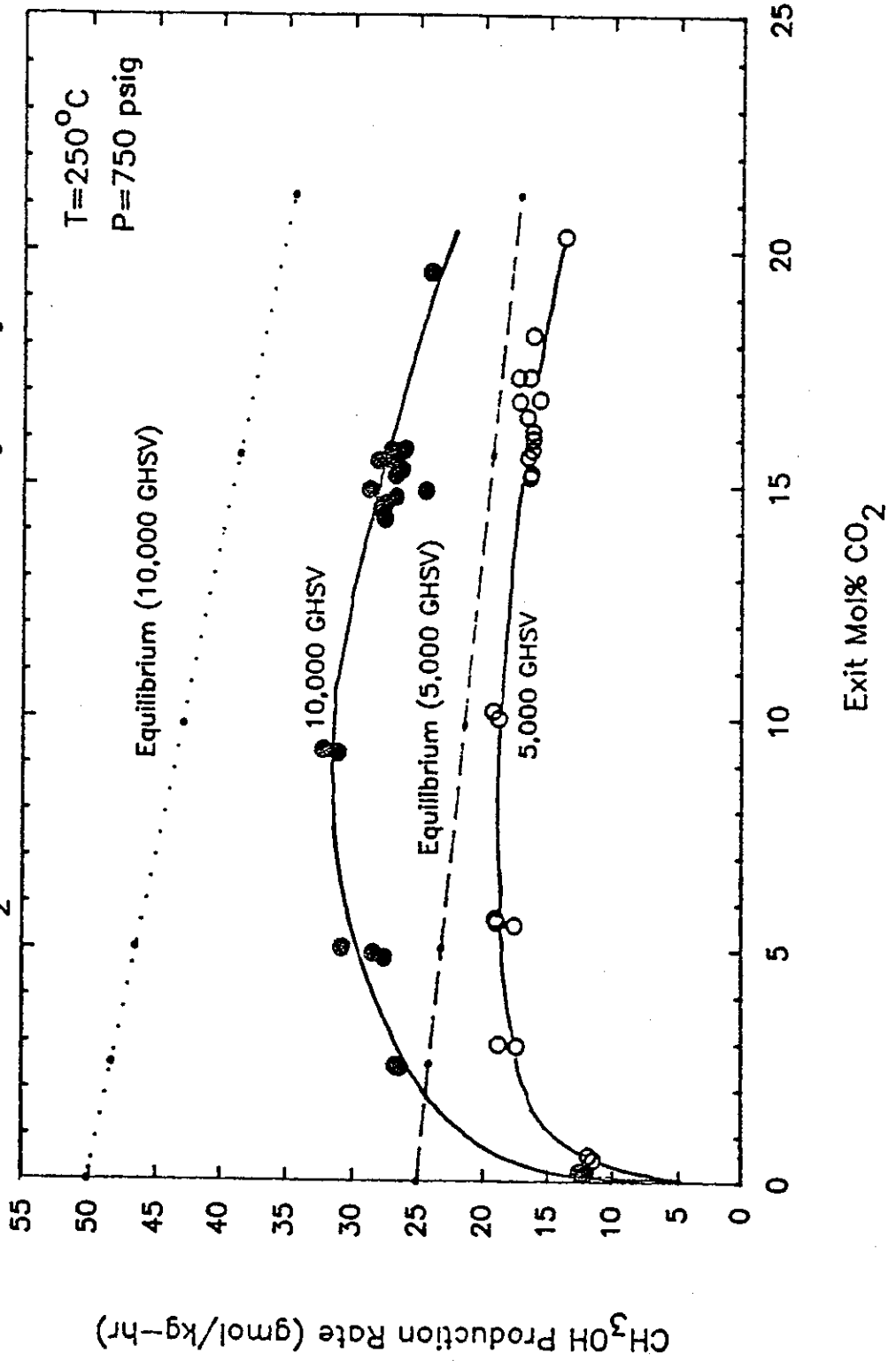


FIGURE 6: The dependence of CH_3OH production rate on feed H_2O concentration for CO -rich gas (13% CO_2).

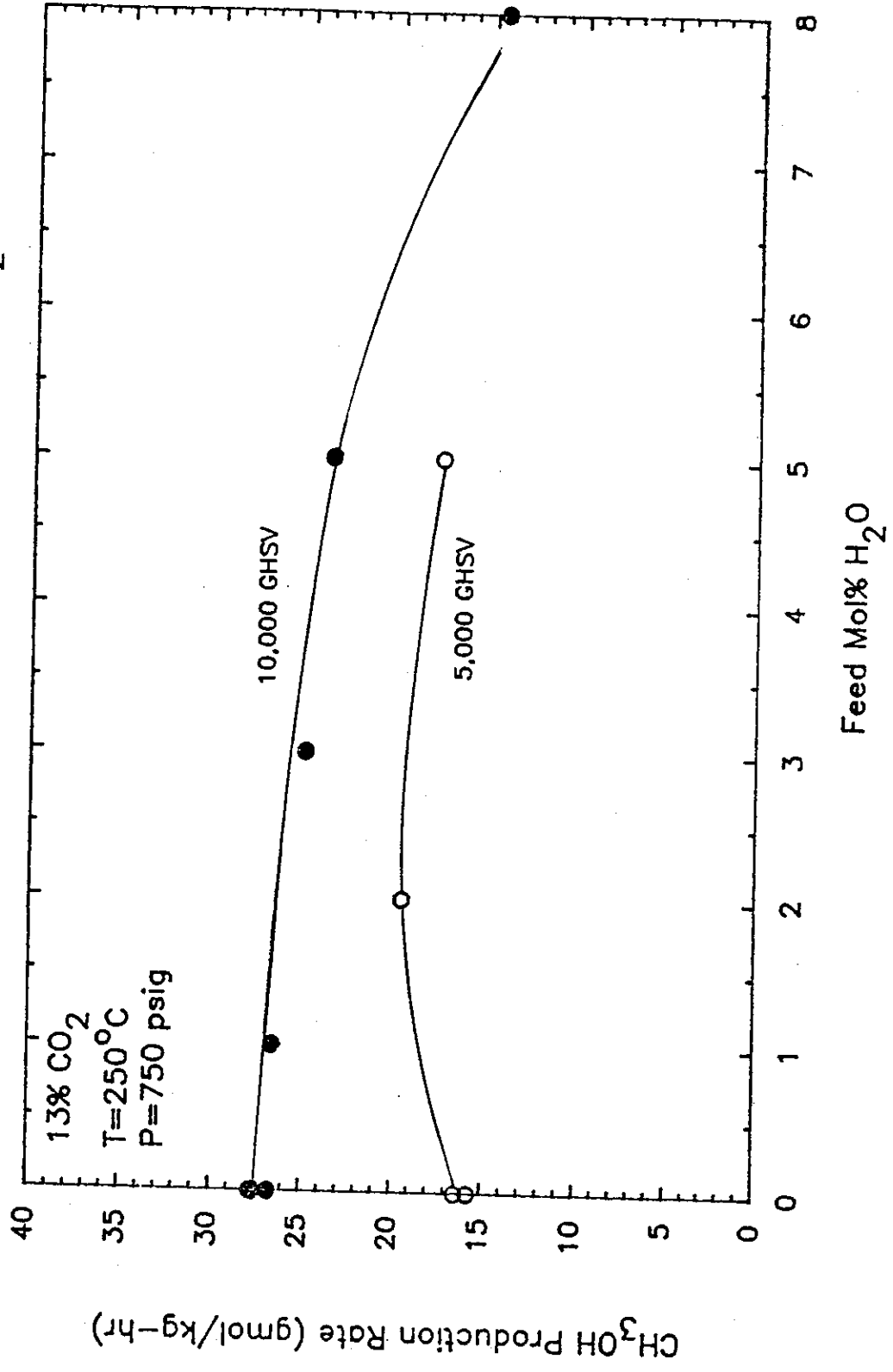


FIGURE 7: The dependence of CH_3OH production rate on feed H_2O concentration for 0% CO_2 feed gas.

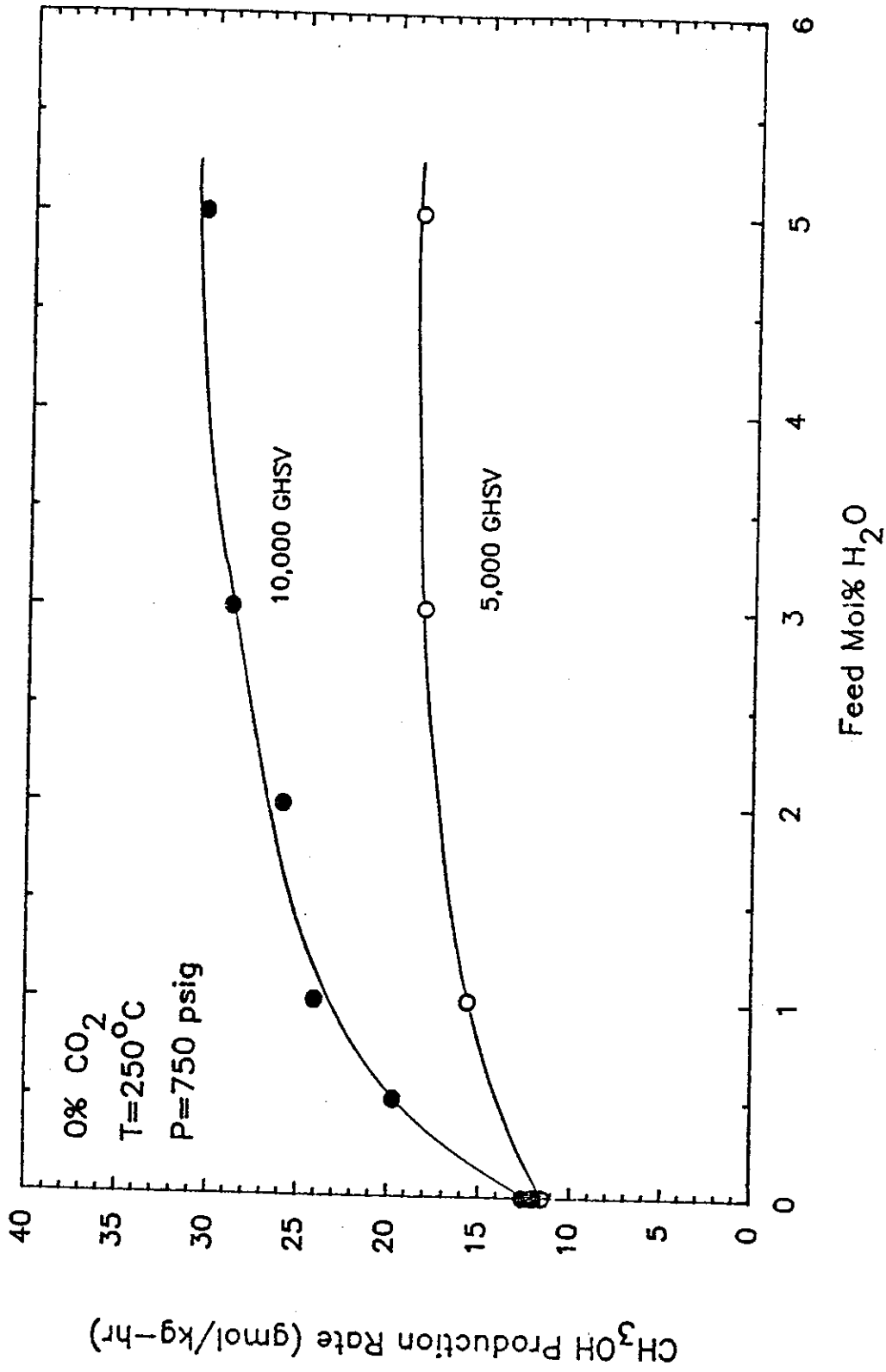


FIGURE 8: The dependence of CH_3OH production rate on feed H_2O concentration for 0% CO_2 feed gas at 225°C .

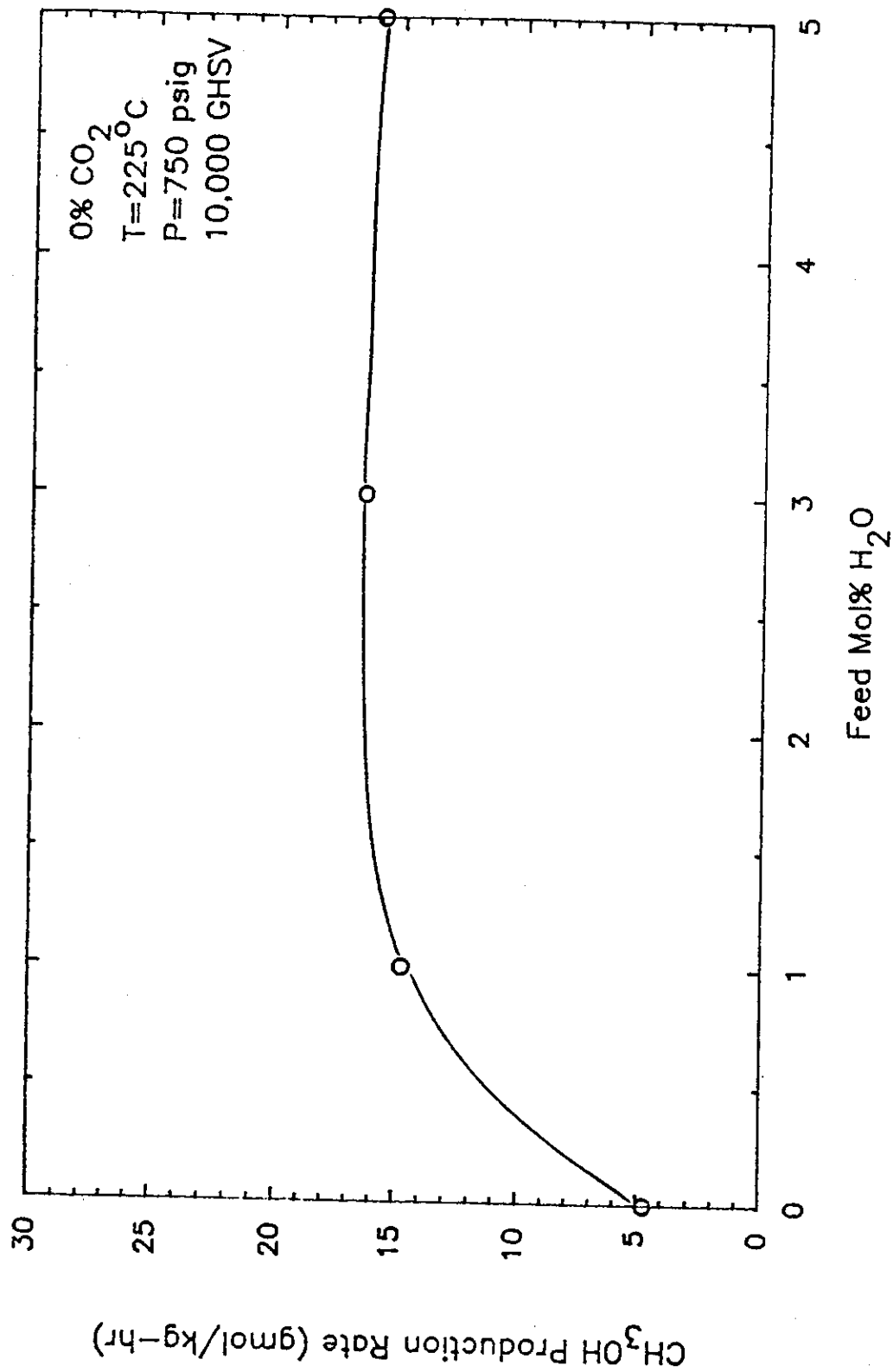


FIGURE 9: The dependence of CH_3OH production rate on feed H_2O concentration for the 4% CO_2 feed gas.

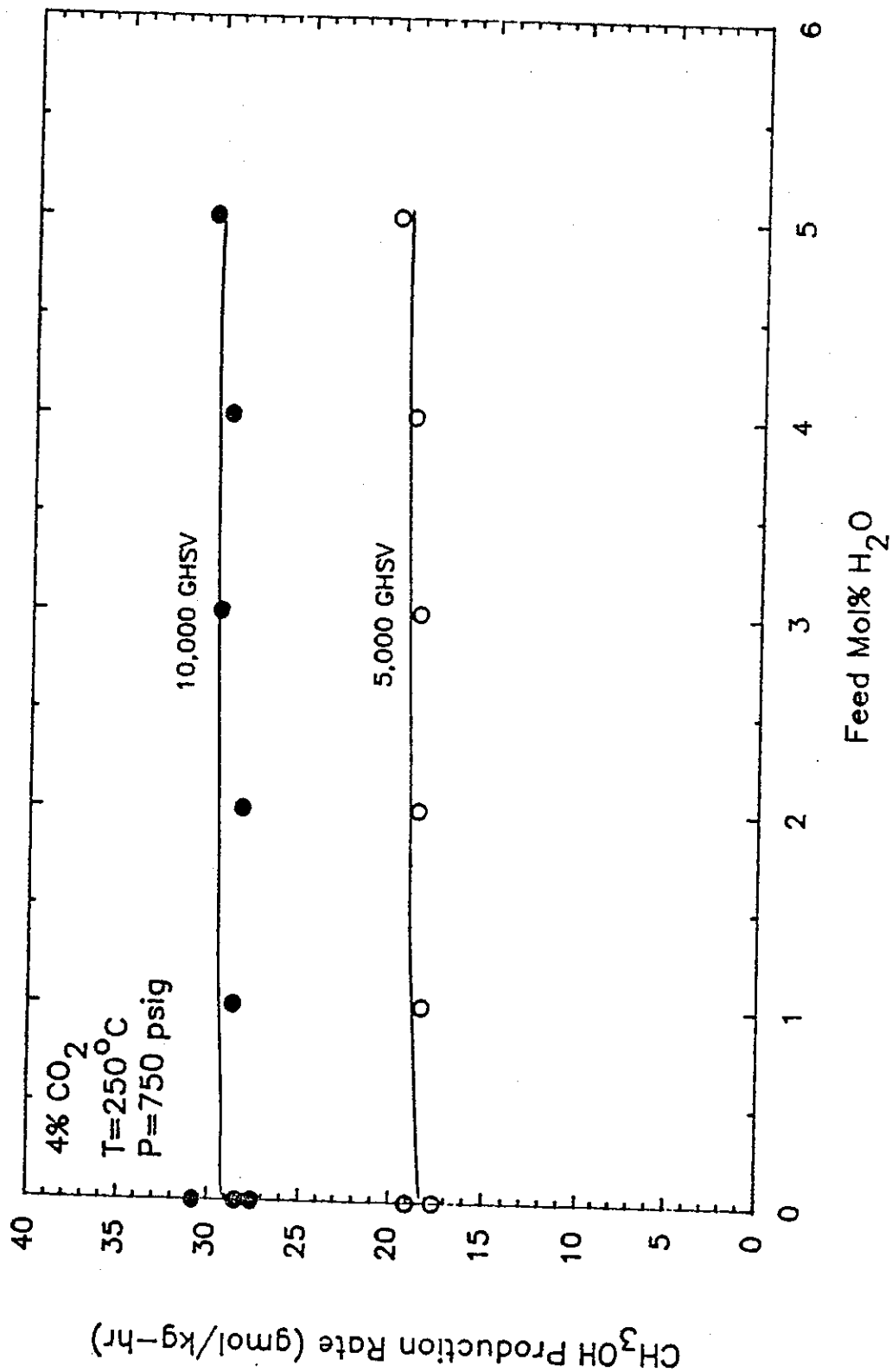


FIGURE 10: The dependence of CH_3OH production rate on feed H_2O concentration for the 8% CO_2 feed gas.

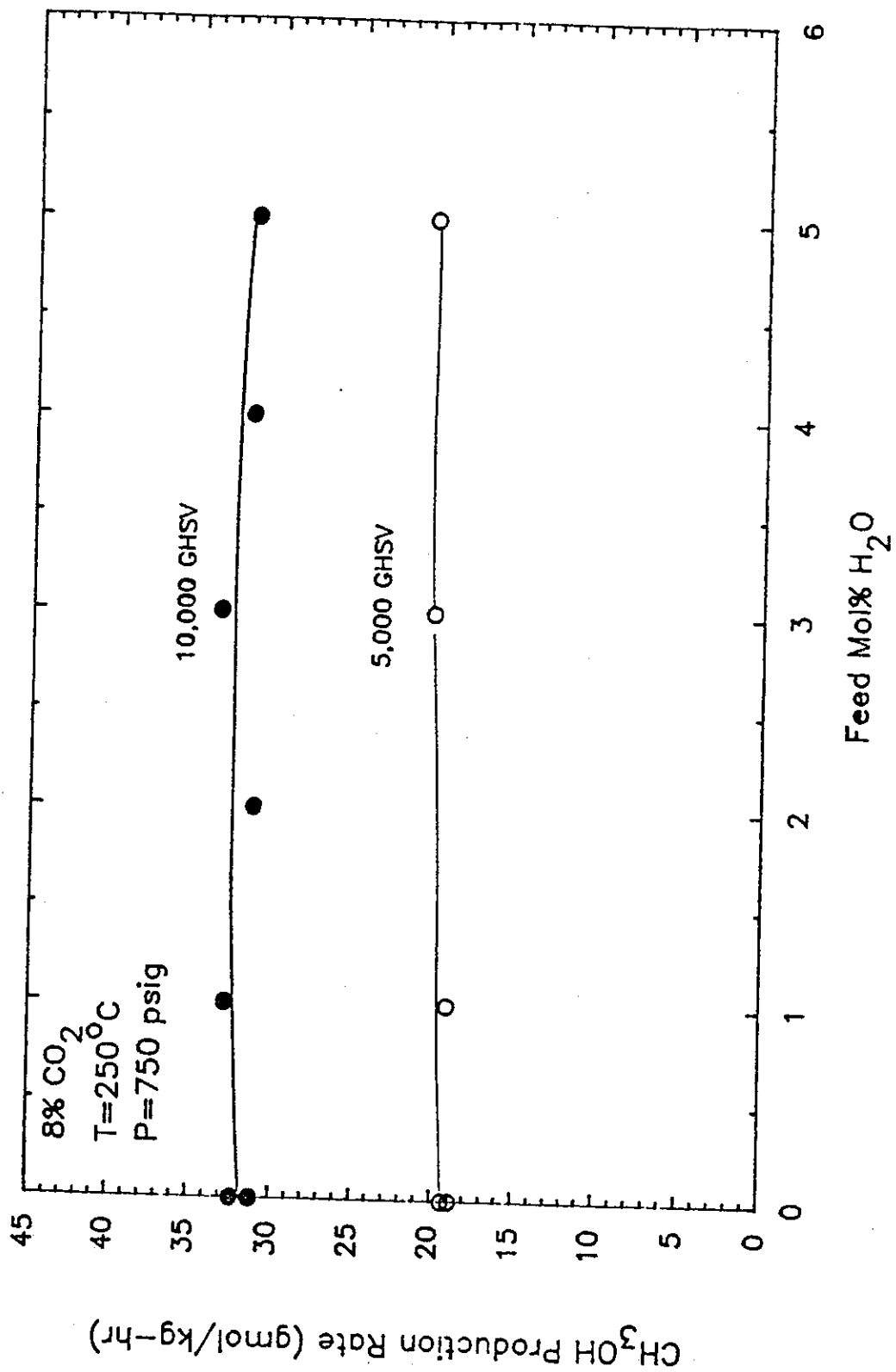


FIGURE 11: The dependence of CH_3OH production rate on the feed H_2O concentration for Shell gasifier gas.

